Response to the reviewer:

We sincerely thank the reviewers for their insightful feedback and constructive suggestions, which have significantly improved our manuscript. Our detailed responses to each comment are provided below, with reviewer comments in black and our responses in blue. We have included the relevant revised text to show how each suggestion has been incorporated.

Comments

1. *Firstly, although the title and Methods emphasize the CNN-LSTM model, it is used solely for outlier replacement. The manuscript does not yet demonstrate what additional insights the deep learning approach offers beyond conventional gap-filling techniques such as linear regression or random forest. The authors are encouraged to supply a comparison table that shows the CNN-LSTM's performance relative to other simpler methods. It might also be helpful to conduct an independent cross-validation, for example, leave-one-site-out to confirm that the network reproduces physically meaningful variability rather than site-specific bias.*

Response：We sincerely thank you for your attention to our research and the valuable comments you have provided. Regarding the questions you mentioned about the application scope of the CNN-LSTM model and its comparison with other methods, we deeply agree and have made the following supplements and modifications:

(1) Comparison with Conventional Gap-filling Techniques

In the revised manuscript, we have added "3.1.1 Comparison with Conventional Gap-filling Techniques", comparing the CNN-LSTM model with traditional methods such as linear regression, random forest, and K-nearest neighbors. As shown in **Table 2**, the CNN-LSTM model performs better in terms of MAE, RMSE, and R^2 metrics. The specific manuscript revision is located at **Lines 243-273**.

Table 2. Comparison of MAE, RMSE, and R^2 among different models.

Model Type	MAE（μg·m^{-3}）	RMSE（μg·m^{-3}）	R^2
Linear Regression	12.6852	17.8804	0.8028
RF	14.6494	20.0135	0.8482
KNN	15.6263	24.2398	0.8135
CNN-LSTM	12.6705	17.4935	0.8840

(2) Ablation Study of CNN-LSTM

Thanks for the valuable suggestions from the reviewer. To more comprehensively validate the performance and reliability of the CNN-LSTM model, we have conducted detailed ablation experiments in the supporting materials and optimized the cross-validation methods. In **Section S1 "Ablation Study of CNN-LSTM"** of the supplement, we systematically removed or modified key components of the model to evaluate their individual contributions to overall performance. The specific experimental results are shown in **Table S1**:

Table S1. Performance Comparison of MAE, RMSE, and R^2 across Model Variants.

Model Type	MAE（μg·m^{-3}）	RMSE（μg·m^{-3}）	R^2
CNN	14.7668	19.2806	0.8591
LSTM	14.3056	21.1303	0.8308
CNN-LSTM	12.6705	17.4935	0.8840

CNN-only model： The CNN-only model using only convolutional layers without LSTM components achieved an MAE of 14.7668 μg·m^{-3}， RMSE of 19.2806 μg·m^{-3}, and R^2 of 0.8591. This configuration can effectively extract spatial features from input data, but due to the lack of temporal modeling, compared to the complete CNN-LSTM model, the MAE increased by 16.54%.

LSTM-only model： The LSTM-only configuration using only recurrent layers without convolutional preprocessing achieved an MAE of 14.3056 μg·m^{-3}， RMSE of 21.1303 μg·m^{-3}, and R^2 of 0.8308. Although the LSTM component successfully captured temporal dependencies, the lack of spatial feature extraction capability led to suboptimal performance, with MAE increasing by 12.90% compared to the complete

model. This result emphasizes the necessity of hierarchical feature extraction when processing complex atmospheric data.

(3) CNN-LSTM model cross-validation

Thanks for the valuable suggestions. Regarding the leave-one-site-out cross-validation, we encountered some data limitation challenges during implementation. Currently, the sample size for each site in our dataset is relatively limited (ranging from 20-70 samples). Direct application of traditional leave-one-site-out validation might affect validation stability due to insufficient data volume at individual sites.

To address this issue, we adopted a site-type-based leave-one-site-out validation strategy. Specifically, we classified all sites in the study area into four types based on their functional characteristics: urban sites, rural sites, urban-rural transition sites, and background sites, then conducted leave-one-site-out cross-validation for each type of site separately. This strategy not only considers the geographical and functional differences of sites but also ensures the stability and reliability of the validation process. In the revised manuscript, we have added "3.1.2 Leave-One-Site-Out Cross-Validation". Through this approach, we can more comprehensively evaluate the model's generalization ability and adaptability to different site types. The specific manuscript revision is located at **Lines 274-302**.

2. *Regarding the source apportionment, PMF analysis is only conducted for four of the twelve sites. The manuscript should explain the basis for this selection. Authors should also include more comprehensive error estimation for the PMF analysis. Authors should expand the diagnostics in Table S3 to report whether > 80% of factor elements are mapped in BS runs, and summarize BS-DISP error estimates.*

Response：Thank you for your valuable comments regarding the PMF analysis. We appreciate your thorough review and constructive suggestions.

The selection of these four sites was based on the following considerations: First, these four sites possess good representativeness in terms of geographical location and environmental characteristics. Second, considering the data quality requirements for PMF model analysis, we selected sites with high data completeness and reliability. Specifically, Nanning represents the southern inland urban environment (located relatively close to the coast), Longfengshan is located in the northeastern region and serves as a background site reference, Zhengzhou, as an important transportation hub, exhibits typical suburban characteristics, and Gucheng is situated in the key pollution area of the Beijing-Tianjin-Hebei region, representing the rural environmental characteristics of this area. We have added detailed explanations for the site selection criteria in the revised manuscript (**Lines 451-458**): "This study employed the PMF model to conduct a detailed analysis of PM_{10} sources at four representative sites selected based on distinct geographical and environmental characteristics. The selection criteria considered regional representativeness, pollution characteristics, and geographical diversity across China. The selected sites include: NN, an urban site in southern China with coastal proximity; LFS, a remote site located in the northeastern region of Heilongjiang Province; ZZ, a suburban site serving as a major transportation hub in central China; and GC, a rural site situated in the heavily polluted Beijing-Tianjin-Hebei region. These four sites collectively represent different pollution source characteristics and regional environmental conditions, enabling a comprehensive understanding of PM_{10} source apportionment across diverse geographical and climatic zones in China."

Regarding the expanded diagnostics with PMF results, we expanded Table S3 to include both the percentage of factor elements successfully mapped in Bootstrap (BS) runs with explicit indication of whether the >80% threshold is met for each factor, and comprehensive BS-DISP error estimates. The determination of optimal factor number was guided by Q_{true}/Q_{robust} values and BS mapping evaluation, as demonstrated in Figure S1.

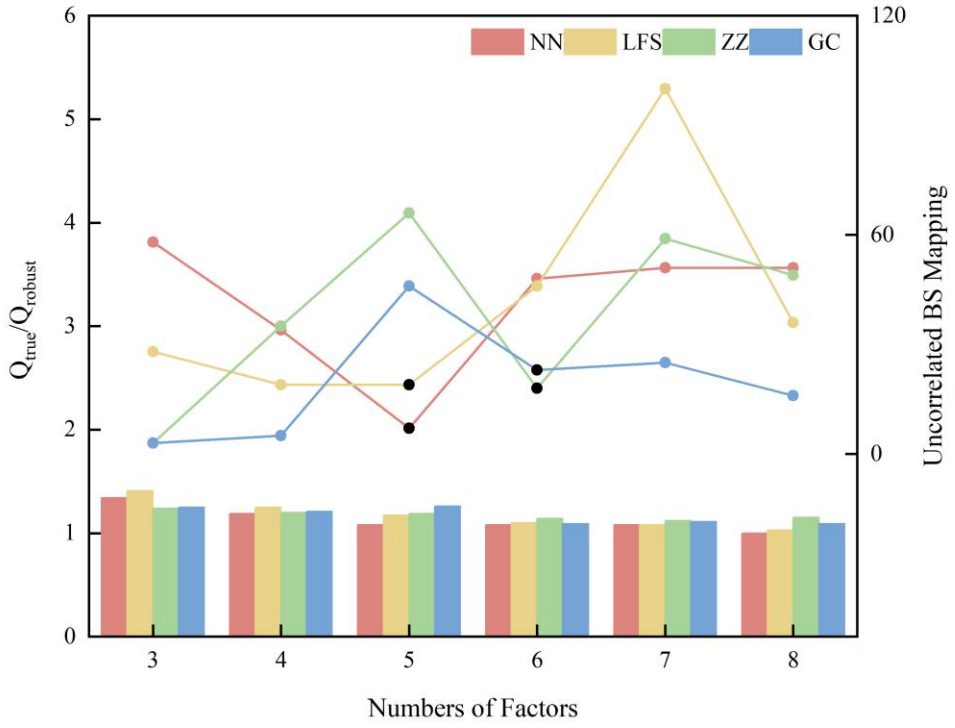

Figure S1. Changes in Q_{true}/Q_{robust} and uncorrelated bootstrap (BS) mapping calculated by the PMF model for varying numbers of factors (3-8). Black dots represent the optimum solution factors at each station.

Table S3. Summary of error estimation diagnostic with PMF at NN, LFS, ZZ and GC station.

Diagnostics		NN	LFS	ZZ	GC
	Number of base run	20	20	20	20
	Q_{robust}	2338	2658.86	2043.86	2066.75
	Q_{true}	2521.1	3160.89	2341.26	2249.16
	Q_{true}/Q_{robust}	1.08	1.18	1.14	1.09
DISP	% dQ	< 0.1 %	< 0.1 %	< 0.1 %	< 0.1 %
	swaps	0	0	0	0
BS	Number of run	100	100	100	100
	Extra modeling uncertainty (%)	0	0	0	0
	Min. Correlation R-Value	0.6	0.6	0.6	0.6
	Mapping	Dust: 94% Biomass burning: 99% Others: 100%	Secondary aerosol: 88% Traffic: 97% Agricultural activities:95% Others: 100%	Coal combustion: 87% Secondary aerosol: 97% Agricultural activities: 98% Others: 100%	Agricultural activities: 90% Coal combustion: 85% Others: 100%
BS-DISP	#of Cases Accepted	89	78	80	71
	% cases with swaps	9%	18%	15%	25%

3. *Furthermore, the discussion on OP lacks depth. OP_v reflects a combination of PM mass concentration and particle intrinsic toxicity. The current discussion on OP focuses almost exclusively on emissions. Authors are encouraged to discuss how emission sources influence OP_v differently from their share of PM_{10} mass. For example, integrating Fig. 11 and Fig. 12 will help to reveal the intrinsic toxicity associated with different emission sources.*

Response： **We appreciate the reviewer's insightful comment regarding the need for deeper discussion on OP.** In response to this valuable feedback, we have substantially revised Section 3.4.2 Source apportionment of OP in PM_{10} (**Lines 565-669**) to address the intrinsic toxicity of different emission sources beyond their mass contributions. Specifically, we now discuss the mass-normalized oxidative potential (OP_m) for each emission source, which reveals how sources contribute to OP_v differently from their share of PM_{10} mass. The analysis revealed significant variations in toxic efficiency among different sources, with traffic emissions showing consistently high OP_m values (0.013-0.022 nmol $H_2O_2 \cdot \mu g^{-1}$) across all sites, while biomass burning exhibited site-specific patterns with notable contributions at NN and GC sites but zero oxidative potential contributions at LFS and ZZ sites despite mass contributions. Secondary aerosols, coal combustion, agricultural activities, and dust sources also demonstrated substantial spatial variations in toxic efficiency, highlighting the complex relationship between source contributions and intrinsic toxicity.

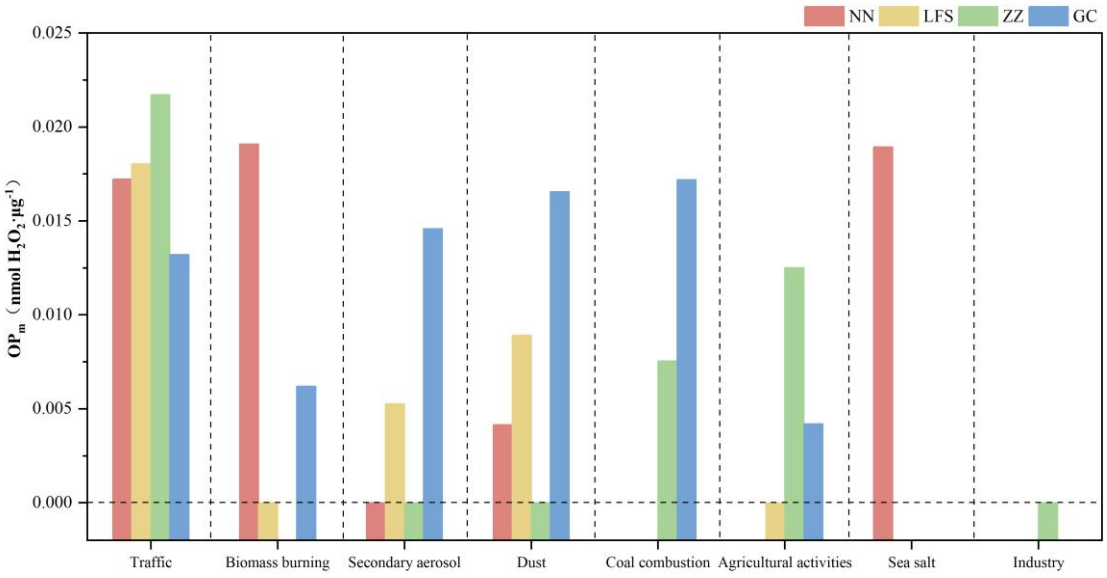

Figure 11. Comparison of OP_m contributions from different emission sources across NN, LFS, ZZ and GC sites.

Specific comments:

4. *#33, "due to its small particle size", this statement does not seem valid for PM_{10}.*

Response: We are very sorry for our careless mistake. We have revised this statement by removing the reference to "small particle size" and now state in **Lines 32-34**: "PM_{10} can remain suspended in the atmosphere for extended periods of time, significantly affecting atmospheric visibility while potentially exerting profound effects on regional and global climate change through both direct and indirect mechanism (Slanina and Zhang, 2004)."

5. *#62, photochemical aging can either decrease or increase OP, for example, this paper reports a decrease after O_3 aging: Ma, S., Cheng, D., Tang, Y., Fan, Y., Li, Q., He, C., Zhao, Z. and Xu, T., 2025. Investigation of oxidative potential of fresh and O_3-aging $PM_{2.5}$ from various emission sources across urban and rural regions. Journal of Environmental Sciences, 151, pp.608-615.*

Response: Thanks for your valuable comment and for providing the relevant reference. We agree that photochemical aging can have varying effects on the OP of PM, and our original statement was indeed oversimplified. We have revised the

sentence in **Lines 58-61** for: "Significantly, photochemical aging of PM in the atmosphere further alters its OP, possibly related to the formation of secondary organic aerosols, changes in oxidation states of metallic components during the aging process, and the oxidation degree of reactive organic compounds (An et al., 2022; Ma et al., 2025)."

6. *#67-69, this statement is inaccurate. Furthermore, CNN-LSTM is used solely for dealing with missing data, and thus referring to traditional source attribution methods in this context is misleading.*

Response: Thanks for pointing out this important issue. We agree that our original statement could have been misleading. In our study, the CNN-LSTM model is specifically used to handle missing data and anomalies to improve data quality. We have revised the manuscript to make this clear: (1) the CNN-LSTM approach is applied for data preprocessing to ensure high-quality, complete datasets; (2) this data quality improvement step is essential before conducting source apportionment analyses; and (3) we have removed the misleading reference to traditional source attribution methods in this context. The revised text now clearly distinguishes between data quality improvement (using CNN-LSTM) and subsequent source apportionment analyses, providing a more accurate representation of our methodology. The detailed revisions can be found in **Lines 63-80** of the revised manuscript.

"However, an accurate assessment of the health risks associated with PM_{10} requires an accurate analysis of its sources and chemical compositions. High-quality, complete datasets are essential for reliable source apportionment and subsequent risk assessment. Environmental monitoring data often contain missing values and anomalies due to instrument malfunction, maintenance periods, or extreme weather conditions, which can significantly affect the accuracy of subsequent analyses. In recent years, with the rapid development of deep learning technology, its application in handling environmental data quality issues has received increasing attention. Deep learning models, particularly the combination of Convolutional Neural Networks (CNN) and Long Short-Term Memory networks (LSTM), have demonstrated

significant advantages in identifying and correcting anomalies and filling missing values in time series environmental data. CNNs effectively extract spatial features, while LSTMs excel at capturing long-term dependencies in time series (Huang and Kuo, 2018; Li et al., 2020). This hybrid model not only identifies anomalies, but also improves data completeness and reliability by predicting and replacing anomalous or missing values (Lee et al., 2019; Qin et al., 2019). Compared with traditional machine learning methods, CNN-LSTM models show superior performance in several evaluation metrics, such as Mean Absolute Error (MAE), Root Mean Square Error (RMSE) (Huang and Kuo, 2018; Yang et al., 2020a; Li et al., 2020). CNN-LSTM models retain significant value in processing atmospheric particulate matter data for data quality improvement. Their spatial feature extraction capabilities effectively identify and correct anomalies caused by instrument malfunction or local pollution events, thereby improving data quality (Zhang and Zhou, 2023). Through training and learning, CNN-LSTM models can effectively predict and fill missing data, providing a high-quality data foundation for subsequent source apportionment and risk assessment analyses (Li et al., 2020; Yang et al., 2020a)."

7. #190-191, the criterion for flagging outliers appears arbitrary. The summed species exceeding the measured PM_{10} mass does not necessarily indicate outliers considering measurement uncertainties.

Response：We sincerely appreciate your insightful reflections and valuable suggestions regarding the quality control standards of this study.

Due to our oversight during the final manuscript preparation, the text incorrectly stated OM =1.4*OC in **Line 326**, but we actually used OM = 1.2*OC throughout all our calculations and data analysis. We have carefully reviewed our analysis code and confirmed that 1.2 was consistently applied. This discrepancy has now been corrected in the revised manuscript. On the closure between chemical components and PM_{10} mass concentration, this study adopted a conservative OM/OC ratio of 1.2 for organic matter estimation. This approach was based on the following considerations:

This study primarily analyzed chemical components including OC, EC, and water-soluble ions (constituting major PM_{10} constituents). However, due to experimental limitations, metal elements and water-insoluble components were not included in the analysis.

For OM estimation, we deliberately adopted the smaller conversion factor of 1.2 as recommended in the literature. Classical studies including White and Roberts have established that 1.2-1.4 represents a conservative range commonly used in mass balance analyses (White and Roberts, 1977). Therefore, by employing the minimum conversion factor (1.2) while excluding certain components, the sum of our 11 measured chemical species should theoretically not exceed the total PM_{10} mass concentration. This approach aligns with standard practices in aerosol characterization research. We fully appreciate the reviewer's rigorous perspective and will strive to incorporate additional component measurements in future studies.

Regarding the classification of samples with chemical component sums below 50% of PM_{10} mass as outliers, we maintain this represents a conservative quality control criterion. Di et al. shown that Chongqing study demonstrated that carbonaceous components alone accounted for 33-35% of PM_{10} mass (Di et al., 2007). Furthermore, research conducted in Luohe City from May 2017 to February 2018 showed that nine water-soluble ions (F^-, Cl^-, NO_3^-, SO_4^{2-}, NH_4^+, Ca^{2+}, Na^+, Mg^{2+}, K^+) comprised an average of 35.67% of PM_{10} mass (Wang et al., 2018). In this study, we analyze 11 components primarily encompassing both carbonaceous fractions and water-soluble ions.

We therefore consider the 50% threshold for chemical component summation to be scientifically justified. However, we acknowledge potential limitations in this approach, as natural conditions might legitimately produce PM_{10} compositions where these measured components constitute less than 50% of total mass. In subsequent research, we will incorporate auxiliary data including meteorological conditions and local pollution source distributions to better evaluate whether sub-threshold measurements truly represent outliers.

Reference

Di, Y., Qi, Z., Changtan, J., Jun, C., and Xiaoxing, M.: Characteristics of elemental carbon and organic carbon in PM_{10} during spring and autumn in Chongqing, China, China Particuology, 5, 255-260, https://doi.org/10.1016/j.cpart.2007.03.009, 2007.

Liu, Y., Zhang, W., Yang, W., Bai, Z., and Zhao, X.: Chemical Compositions of $PM_{2.5}$ Emitted from Diesel Trucks and Construction Equipment, Aerosol Science and Engineering, 2, 51-60, https://doi.org/10.1007/s41810-017-0020-2, 2018.

Lodovici, M. and Bigagli, E.: Oxidative Stress and Air Pollution Exposure, Journal of Toxicology, 2011, https://doi.org/10.1155/2011/487074, 2011.

Wang, N., Yin, B., Wang, J., Liu, Y., Li W., Geng, C., and Bai, Z.: Characteristics of Water-Soluble lon Concentration Associated with PM_{10} and $PM_{2.5}$ and Source Apportionment in Luohe City Research of Environmental Sciences, 31, 2073-2082, https://doi.org/10.13198/j.issn.1001-6929.2018.08.18, 2018.

White, W. H. and Roberts, P. T.: On the nature and origins of visibility-reducing aerosols in the los angeles air basin, Atmos. Environ., 11, 803-812, https://doi.org/10.1016/0004-6981(77)90042-7, 1977.

8. *#331, which six monitoring stations are being referred to?*

Response: **We thank the reviewer for this important clarification request.** Upon revisiting the data, we realized that the initial phrasing could be more precise regarding the number of monitoring stations. In the revised manuscript (**Lines 368-369**), we have clarified the text as follows: "Five monitoring stations including GC, LFS, DH, LA, and Nanning (NN) exhibited significantly elevated concentrations during spring, which can be attributed to multiple factors."

9. *#353-355, any reference that supports the temperature-dependent partitioning of ammonium sulfate?*

Response： **Thanks for your valuable suggestions.** We have added a reference that document the temperature dependence of ammonium sulfate partitioning behavior in **Lines 390-392**: "Furthermore, the relatively lower temperatures in winter facilitate

the gas-to-particle conversion of gaseous precursors, promoting the partitioning of semi-volatiles such as ammonium sulfate and ammonium nitrate to the particulate phase (Wang et al., 2020)."

Reference

Wang, M., Kong, W., Marten, R., He, X.-C., Chen, D., Pfeifer, J., Heitto, A., Kontkanen, J., Dada, L., Kürten, A., Yli-Juuti, T., Manninen, H. E., Amanatidis, S., Amorim, A., Baalbaki, R., Baccarini, A., Bell, D. M., Bertozzi, B., Bräkling, S., Brilke, S., Murillo, L. C., Chiu, R., Chu, B., De Menezes, L.-P., Duplissy, J., Finkenzeller, H., Carracedo, L. G., Granzin, M., Guida, R., Hansel, A., Hofbauer, V., Krechmer, J., Lehtipalo, K., Lamkaddam, H., Lampimäki, M., Lee, C. P., Makhmutov, V., Marie, G., Mathot, S., Mauldin, R. L., Mentler, B., Müller, T., Onnela, A., Partoll, E., Petäjä, T., Philippov, M., Pospisilova, V., Ranjithkumar, A., Rissanen, M., Rörup, B., Scholz, W., Shen, J., Simon, M., Sipilä, M., Steiner, G., Stolzenburg, D., Tham, Y. J., Tomé, A., Wagner, A. C., Wang, D. S., Wang, Y., Weber, S. K., Winkler, P. M., Wlasits, P. J., Wu, Y., Xiao, M., Ye, Q., Zauner-Wieczorek, M., Zhou, X., Volkamer, R., Riipinen, I., Dommen, J., Curtius, J., Baltensperger, U., Kulmala, M., Worsnop, D. R., Kirkby, J., Seinfeld, J. H., El-Haddad, I., Flagan, R. C., and Donahue, N. M.: Rapid growth of new atmospheric particles by nitric acid and ammonia condensation, Nature, 581, 184-189, https://doi.org/10.1038/s41586-020-2270-4, 2020.

10. *#365-366, the high OP_v in Gucheng is related to its high PM_{10} mass concentration.*

Response: Thanks for your insightful comment. We agree that the high OPv levels in Gucheng are indeed related to its high PM_{10} mass concentration. We have revised the manuscript to explicitly acknowledge this important relationship and highlight the correlation between particulate matter loading and OP_v levels at this site. The revised text now emphasizes that the elevated OP_v concentrations are consistent with the high PM_{10} concentrations observed, while also considering the regional pollution characteristics and transport effects. This revision strengthens our interpretation of the data and provides a more comprehensive explanation for the observed patterns. We have revised in **Lines 401-406**: "However, the study revealed unexpectedly high average OP_v levels at the rural site in GC, ranking second highest among all sites. This finding is consistent with the high PM_{10} mass concentrations observed at this site, suggesting a strong correlation between particulate matter loading and OP_v levels. GC,

located in the Beijing-Tianjin-Hebei region characterized by high population density and typical pollution concentration, experiences elevated OP_v levels likely due to the combined influence of high PM_{10} concentrations, pollutant transport from surrounding urban areas, and local emissions (Han et al., 2015)."

11. *3.4, 3.4.1, 3.4.2 source appointment should be source apportionment.*

Response: Thanks for your careful review. We feel sorry for our carelessness. We have corrected in **Lines 449, 450, and 565** as follows: "3.4 Source apportionment", "3.4.1 Source apportionment of PM_{10}", "3.4.2 Source apportionment of OP in PM_{10}".

12. *#471, Liu et al. 2023 is cited in the text but missing from the reference list.*

Response: We are sorry for the confusion. We have rewritten the discussion content in that section, adding new, more appropriate references to better support our arguments. We have verified that all the citations in the revised manuscript correspond to the entries in the reference list in **Lines 522-526**: "The sixth factor had high levels of K^+ (60.6%), Ca^{2+} (38.4%), EC (39.3%), OC (28.8%), and NO_3^- (25.0%), based on comprehensive analysis of these characteristic species, this factor may be related to agricultural activity emissions, contributing approximately 22% to PM_{10}. Ca^{2+}, OC and EC may be related to surface soil dust (Yu and Cao, 2023), Jung et al. found elevated K^+ concentrations at schools near corn farms, supporting the agricultural source attribution (Jung et al., 2024), while NO_3^- would be related to fertilizer application (Cao et al., 2018)."

Reference

Cao, P., Lu, C., and Yu, Z.: Historical nitrogen fertilizer use in agricultural ecosystems of the contiguous United States during 1850–2015: application rate, timing, and fertilizer types, Earth Syst. Sci. Data, 10, 969-984, https://doi.org/10.5194/essd-10-969-2018, 2018.

Jung, C., Huang, C., Su, H., Chen, N., and Yeh, C.: Impact of agricultural activity on $PM_{2.5}$ and its compositions in elementary schools near corn and rice farms, Sci. Total Environ., 906, 167496, https://doi.org/10.1016/j.scitotenv.2023.167496, 2024.

Yu, Y. and Cao, J.: Chemical Fingerprints and Source Profiles of PM_{10} and $PM_{2.5}$ from Agricultural Soil in a Typical Polluted Region of Northwest China, Aerosol Air Qual. Res., 23, 220419, https://doi.org/10.4209/aaqr.220419, 2023.

13. *Figure 10, The agricultural activities factor shows very different OC/EC loadings at ZZ vs. GC. Please provide supporting literature or discuss why the profiles are different.*

Response: Thank you for your valuable comment. This difference can be attributed to regional agricultural practices: The suburban ZZ site (Zhengzhou) is located in an intensively cultivated area with high agricultural mechanization, while the rural GC site (Gucheng, Baoding) represents a more traditional farming area. We have analyzed the different OC/EC loadings in the agricultural activities factor between ZZ and GC and added the following discussion in the revised manuscript in **Lines 548-553**: "The contrasting OC/EC loadings in the agricultural activities factor between the suburban ZZ site and rural GC site reveal important insights into the spatial heterogeneity of agricultural emissions. The suburban ZZ site, located in the intensively cultivated Central Plains, experiences higher carbonaceous aerosol loadings from mechanized farming operations, which contribute significantly to EC emissions through diesel exhaust from agricultural machinery (Liu et al., 2018). In contrast, the rural GC site in Baoding represents areas with traditional, less mechanized farming practices, resulting in minimal EC contributions from agricultural activities."

14. *#510-512, please clarify what pathways.*

Response: Thanks for your suggestion. We have added in **Lines 651-652**: "NO_3^- formed during fertilizer application can influence particle oxidative properties through ionic strength effects and acidification processes (Lodovici and Bigagli, 2011)"

15. *#526-529, these statements are inconsistent with the results in Fig. 12. In GC, the contribution of coal combustion to OP_v ranks second among the four sites, and the*

secondary aerosols contribution at GC is smaller than LFS. Please re-examine the conclusions.

Response: **Thank you for pointing out this inconsistency and we apologize for any confusion caused.**

We have made substantial revisions to Section 3.4.2 (**Lines 565-669**). In this section, we have conducted a mass-normalized OP analysis to evaluate the intrinsic oxidative potential of particles from different emission sources more effectively. Specifically, we have compared and discussed the contribution of OP concentrations in a unit mass of PM_{10} from each emission source across the NN, LFS, ZZ and GC sites. This mass-normalized approach allows us to distinguish between the effects of particle mass concentration and the inherent oxidative potential of particles from different sources, providing a more accurate assessment of source-specific toxicity. The detailed analysis and discussion can be found in the revised Section 3.4.2 (**Lines 565-669**).